

# Three-phase Unbalance Warning Control Scheme for Circuits Based on Current Sensor Data Acquisition

Qingchan Liu,<sup>1,2</sup> Yuang Lin,<sup>3\*</sup> and Yao Zhong<sup>1,2</sup>

<sup>1</sup>Metrology Center of Yunnan Power Grid Co., Ltd., Kunming 650200, P.R. China

<sup>2</sup>Yunnan Provincial Power Load Control Technology Center, Kunming 650200, P.R. China

<sup>3</sup>Faculty of Information Engineering and Automation, Kunming University of Science and Technology, Kunming 650500, P.R. China

(Received May 22, 2023; accepted October 16, 2023)

**Keywords:** three-phase four-wire distribution network, current sensor, QPSO-LSTM network, three-phase unbalance warning and control

Three-phase unbalance is a major factor causing faults in three-phase four-wire distribution network systems, which can result in a significant decline in power quality, reduced power conversion efficiency, and other severe consequences. In this study, we present an early warning control scheme for detecting three-phase unbalance in the intelligent distribution sensing terminal of the three-phase four-wire distribution network. The following steps are undertaken. (1) The current sensor module of the intelligent distribution substation sensing terminal realizes the three-phase unbalance calculation of the point current data of the power grid and obtains a time-series dataset of current unbalance rates. (2) The parameters of a long short-term memory (LSTM) network are optimized using the quantum particle swarm optimization (QPSO) algorithm to determine the optimal network layer weights and thresholds during the training of the LSTM network. (3) A QPSO-LSTM-based time-series prediction model is developed to predict the current balance state. The accuracy and feasibility of the model are validated using a time-series dataset of current unbalance rates. (4) The aforementioned steps are integrated to design an early warning control scheme for three-phase unbalance in three-phase four-wire power distribution systems. This comprehensive early warning system enables the early detection and control of three-phase balancing states in the distribution system through the time-series prediction of the current unbalance rate. It facilitates the rotation or replacement of equipment that may disrupt the system's balance, such as aging meters, and the timely detection and response to potential power system attacks. Although the overall early warning system requires a more stable and accurate power data acquisition technology to achieve the desired prediction, the proposed scheme provides valuable insights for controlling and compensating three-phase balancing and monitoring faults in three-phase four-wire circuits.

## 1. Introduction

With the advent of the digital power grid and rising living standards, the electric power system has become an essential infrastructure in modern society. Among the components of the electric

---

\*Corresponding author: e-mail: [18087147030@163.com](mailto:18087147030@163.com)  
<https://doi.org/10.18494/SAM4550>

power system, the three-phase four-wire distribution grid system plays a significant role in the distribution, regulation, and control of electric energy.<sup>(1,2)</sup> This system represents the most prevalent type of power distribution in contemporary power systems, characterized by its simple structure, economic viability, and practicality.<sup>(3)</sup> It finds extensive application in residential areas with low-voltage electricity consumption owing to its ability to minimize line losses and voltage drops during energy transmission, thereby enhancing energy efficiency and power system stability.<sup>(4)</sup> However, in practical applications, the three-phase power system experiences a growing concern of three-phase unbalance due to various factors. This unbalance results in disparities across current, voltage, power, and load within the power system, as well as the hastened aging of the system. These effects, in turn, impact the power metering of intelligent three-phase meters, disrupt the normal operation of the power system, and may even lead to severe power system failures.<sup>(5,6)</sup>

Currently, there is significant research focus on early warning control methods for circuit balance in three-phase four-wire distribution networks. Zheng *et al.* proposed a short-term prediction method for three-phase unbalance management with noise reduction regression.<sup>(7)</sup> Li *et al.* achieved an early warning of three-phase balance through a combined ARIMA-long short-term memory (LSTM) model for voltage time series prediction.<sup>(8)</sup> Zhang *et al.* implemented three-phase current compensation using a current prediction model in the  $\alpha\beta 0$ -coordinate system.<sup>(9)</sup> However, most existing studies<sup>(10–13)</sup> on three-phase balancing control in three-phase four-wire distribution networks primarily rely on current or load monitoring systems for governance.

In summary, various current balance compensation techniques have been developed for three-phase four-wire transformer power balance control, demonstrating a high level of maturity. However, as the current monitoring system only targets all current data for three-phase balancing governance, the compensation technology is often controlled only after the three-phase circuit reaches a state of severe unbalance, which cannot effectively reduce circuit faults caused by severe three-phase unbalance. Moreover, the prediction research of power-quality-related indexes can help achieve an early and timely warning of the balance state of a three-phase circuit, and targeted measures can be taken for balance control to ensure power balance in the long run.

Therefore, in this study, three-phase current data are collected from different levels of transformers, branch boxes, and meter boxes using current sensor modules from intelligent distribution substation sensing, branch line monitoring, and end sensing terminals in a distribution network system.<sup>(14)</sup> A current unbalance rate timing dataset is constructed using a three-phase unbalance calculation model. The established LSTM algorithm is used for current balance timing prediction, and the quantum particle swarm optimization (QPSO) algorithm's stochastic space search property is used for global parameter optimization to improve prediction accuracy. On the basis of the prediction results, an early warning control scheme for three-phase unbalance is designed. This scheme facilitates the rotation of aging equipment, such as smart meters, and can respond in a timely manner to the power system that faces various security threats and attacks, to provide effective situational awareness for deep security defense, minimizing additional losses caused by three-phase unbalance. These findings provide reliable data support and scientific planning suggestions for managing three-phase unbalance in distribution network systems.

## 2. Current Data Collection Based on Intelligent Substation Sensing Terminal

### 2.1 Introduction to three-phase four-wire circuit sensors

In the three-phase four-wire circuit, the state of three-phase unbalance is mainly detected by the power intelligent metering system, which relies on the intelligent collection of terminal data such as voltage, current, and power, and further adopts the three-phase unbalance calculation and three-phase load balancing dynamic planning models to realize the statistics and analysis of three-phase balance data of each node in the distribution network system.

Among them, the three-phase current unbalance can reflect the three-phase unbalanced state of the circuit, mainly relying on current sensors to measure and record current data, for the three-phase four-wire circuit. A schematic diagram of shunt current sensors for the data acquisition line is shown in Fig. 1.

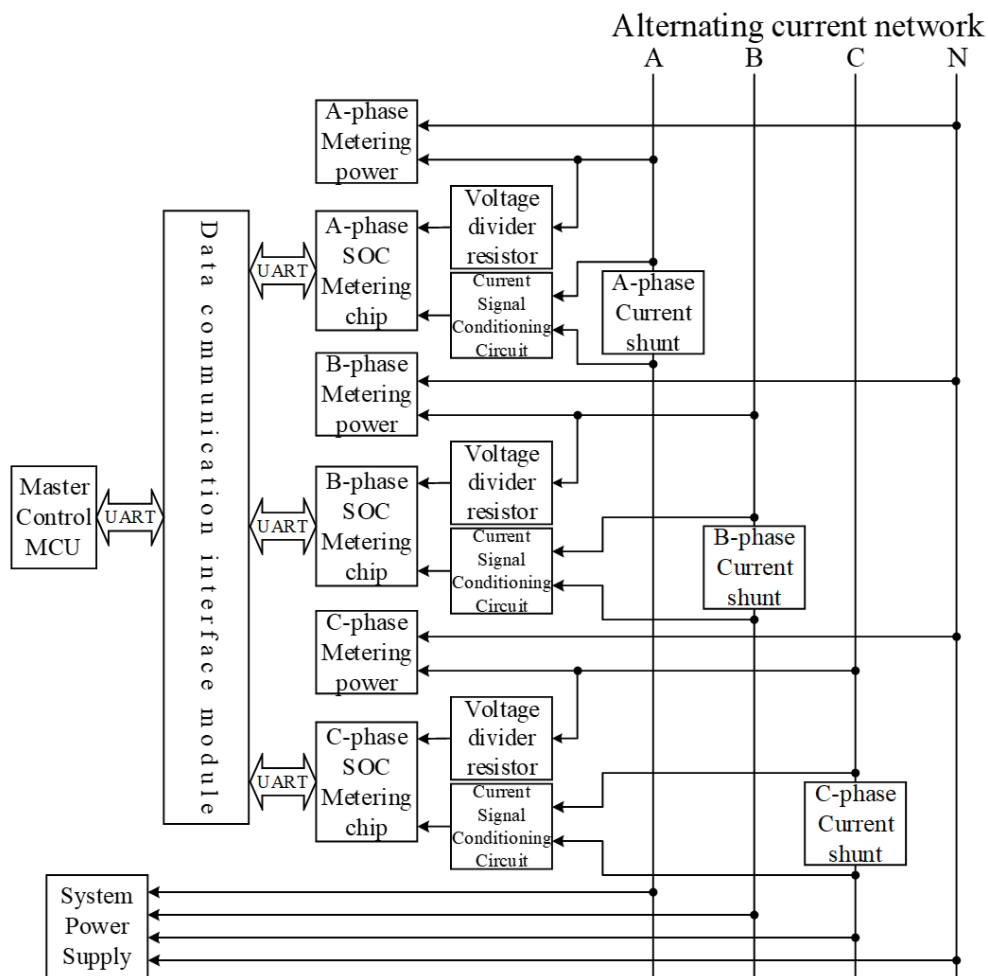


Fig. 1. Schematic diagram of current sensor three-phase data acquisition.

## 2.2 Current balance time-series dataset construction

To enable an early warning of the three-phase unbalance state, it is essential to carry out the time-series prediction of the current unbalance degree and obtain data support for validating the prediction model through simulations. In this study, three-phase current data are gathered using current sensor modules installed in intelligent distribution, branch, and end sensing terminals within a specific station area.

In the three-phase unbalance calculation model, the unbalance degree of the three-phase current is typically determined using two approaches:

$$\mu_I = \frac{I_{max} - I_{min}}{I_{max}}, \quad (1)$$

$$\mu_I = \frac{\max\{I_{A/B/C} - I_{avg}\}}{I_{avg}}. \quad (2)$$

Here,  $I_A$ ,  $I_B$ , and  $I_C$  represent the A, B, and C phase currents, and  $I_{max}$  and  $I_{avg}$  represent the current three-phase maximum and current three-phase average, respectively, and the first more commonly used current unbalance rate calculation method is chosen in this study.

The current data are collected and subjected to preprocessing to obtain the time-series data for current unbalance. For this study, a specific station within a regional smart distribution network is chosen, and the input dataset is derived from the transformer side. The collected current data, representing instances with significant fluctuations in the balance state, are sampled at 15 min intervals to generate the timing data curve for the current unbalance degree. Figure 2 illustrates a portion of this curve.

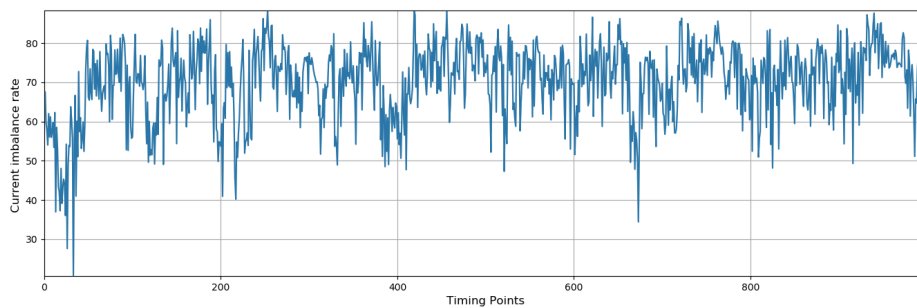


Fig. 2. (Color online) Current unbalance data curve.

### 3. QPSO-LSTM-based Current Balance Prediction Model

#### 3.1 Introduction to long short-term memory network

Conventional neural network structures may not be optimal for predicting power-related data. However, the LSTM, which is an enhanced model derived from the recurrent neural network (RNN), offers improved memory and long-term dependence modeling capabilities. LSTM addresses issues such as gradient disappearance and gradient explosion more effectively.<sup>(15)</sup> LSTM proved to be more suitable for examining the nature of the long sequence of data associated with current balance in this study. The internal structure of LSTM is depicted in Fig. 3.

The LSTM model comprises a fundamental structure that includes a unit state, three gate controllers (input, forget, and output gates), and a memory cell. LSTM has demonstrated excellent performance in modeling temporal data and finds extensive applications in prediction tasks across domains such as finance, meteorology, and electric power.

#### 3.2 Introduction of QPSO algorithm

The particle swarm optimization (PSO) algorithm is a population-based randomized search algorithm.<sup>(16)</sup> However, this algorithm has limitations in terms of the randomness of particle swarm position changes, leading to a restricted search space and a tendency to converge to local minima. To address this issue, the QPSO algorithm was developed, which leverages quantum space to eliminate the directional properties of particles and expand the search space. By doing so, the QPSO algorithm overcomes the premature convergence problem associated with the PSO algorithm.<sup>(17)</sup>

In the D-dimensional space of the quantum particle swarm, the particle population is  $X = (X_1, X_2, \dots, X_m)$ , the position of the  $i$ th individual particle is  $X_i = (X_{i1}, X_{i2}, \dots, X_{ij})^T$ , the particle velocity is  $V_i = (V_{i1}, V_{i2}, \dots, V_{ij})^T$ , the individual optimal solution of the particle object  $i$  is  $P_{best.i} = (P_{best.1j}, P_{best.2j}, \dots, P_{best.ij})^T$ , and the global optimal solution is  $A_{best.i} = (A_{best.1j}, A_{best.2j}, \dots, A_{best.ij})^T$ . We set the number of iterations,  $T$ , the inertia weight  $\lambda$ , and the acceleration coefficient  $c$  with a random number  $r$  from 0 to 1. The changes in the velocity and position of individual particles can be obtained as

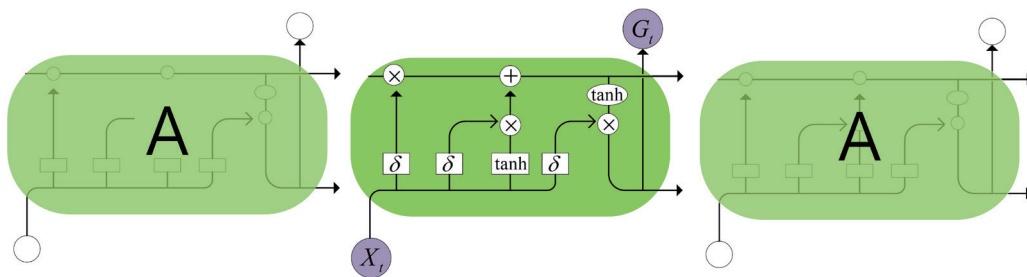


Fig. 3. (Color online) LSTM network model structure diagram.

$$V_{ij}^{T+1} = \lambda V_{ij}^{T+1} + c_1 r_1 (P_{bestij}^T - X_{ij}^T) + c_2 r_2 (A_{bestij}^T - X_{ij}^T), \quad (3)$$

$$X_{ij}^{T+1} = X_{ij}^T + V_{ij}^{T+1}. \quad (4)$$

### 3.3 QPSO-LSTM time series forecasting model

In LSTM network training for temporal prediction, multiple input feature variables are used, while a single variable represents the output. The input information for the current unbalance dataset is derived from the previous time period, and the output represents the subsequent moment's current unbalance. This setup ensures an accurate and reliable short-term balance state prediction.

Within the LSTM network structure, the “forgetting gate” plays a crucial role in determining which information should be discarded from the input data. By processing the previous moment's output, denoted as  $o_{t-1}$ , along with the current moment's input, denoted as  $i_t$ , through the forgetting gate, an  $s_t$  value ranging from 0 to 1 is obtained. This value is then compared with the network layer  $K_{t-1}$  from the previous moment to assess the probability of allowing this portion of information to pass through. When the value is 0, no information is permitted to pass through the gate.

$$S_t = \sigma(w_s \cdot [o_{t-1}, i_t] + v_f) \quad (5)$$

Here,  $\sigma$  is the sigmoid function and  $w_s$  and  $v_s$  are the network weights and thresholds, respectively. Moreover, to determine the information to be saved, the sigmoid structure of the “input gate” layer is used to determine the update of the weights and thresholds, and a new candidate vector  $\tilde{K}_t$  is generated from layer tanh. The new vector is added to the network layer using the following equations:

$$j_t = \sigma(w_i \cdot [o_{t-1}, i_t] + v_i), \quad (6)$$

$$\tilde{K}_t = \tanh(W_k \cdot [o_{t-1}, i_t] + v_k). \quad (7)$$

We update the old network layer  $K_{t-1}$  to  $K_t$ . We multiply  $K_{t-1}$  with  $S_t$ , remove the information that should be forgotten, and add  $j_t * \tilde{K}_t$  to obtain the new network layer  $K_t$ , with the equation

$$K_t = S_t * K_{t-1} + j_t * \tilde{K}_t. \quad (8)$$

Finally, the content output is determined and the output is derived from the updated network layer. The output layer is determined through the sigmoid layer using  $o_{t-1}$  and  $i_t$ . The network layer is then processed through the tanh function and multiplied by the output of the sigmoid layer, and the output  $G_t$  is finally calculated as

$$G_t = \sigma(w_o \cdot [o_{t-1}, i_t] + v_o), \quad (9)$$

$$O_t = G_t * \tanh(K_t). \quad (10)$$

The LSTM network structure is enhanced through the integration of the QPSO algorithm, enabling the determination of optimal weights and thresholds for network layers during training. This is achieved by utilizing the particle random movement search inherent to the QPSO algorithm. Within the quantum space, particles exhibit a movement characterized by a  $P_{best}$ -centered  $\delta$  potential drop towards the center, facilitating convergence within the target range and the exploration for a solution.

During the search process for particles within the quantum space, the simultaneous determination of positions and velocities for different particles is not feasible. The individual states of the optimal search process for each particle are governed by the wave function  $\varphi(B)$ .

$$\varphi(B) = \frac{1}{\sqrt{l}} e^{\frac{-|B|}{l}} \quad (11)$$

By setting the characteristic length of  $\delta$  potential drop to  $l$ , on the basis of the results of Monte Carlo stochastic simulation, the position of the individual particle can be calculated as

$$X = p \pm \frac{l}{2} \ln\left(\frac{1}{a}\right), \quad (12)$$

where  $a$  is a random number in the interval 0 to 1. At moment  $t$ , the position of the individual particle is updated as

$$X(t+1) = p(t) \pm \frac{l(t)}{2} \ln\left(\frac{1}{a}\right). \quad ()$$

By using the mean position  $P_{best}$  of the particle population  $Z_{best}$  and introducing the shrinkage expansion coefficient  $\beta$  with a random number  $\gamma \in [0, 1]$ , in the population size  $M$ , the characteristic length  $l$  can be calculated as

$$Z_{best} = \frac{1}{M} \sum_{m=1}^M P_{best_m}, \quad (14)$$

$$l = 2\beta |X_n - Z_{best}|. \quad (15)$$

By combining the above equations, the updated final particle position is obtained as

$$P_m = \gamma * P_{best_m} + (1 - \gamma) * A_{best}, \quad (16)$$

$$l = 2\beta |X_n - Z_{best}|. \quad (17)$$

Here,  $A_{best}$  is the current global optimal particle, and the individual optimal solution among all particle objects is obtained as  $P_m$ , the particle  $m$  position is  $X_m(t)$ , and the position of the individual particle is updated as  $X_m(t + l)$ . In the training process, when the particle updates its position, the individual and global optimal positions of the particle swarm will also be updated, and the optimal weight and threshold of the LSTM network will be obtained after training.

## 4. Three-phase Current Balance Prediction Based on QPSO-LSTM Model

### 4.1 Algorithm flow

On the basis of the established current balance prediction model, we present in this study the following algorithm flow for specific prediction:

- Step 1: Data preprocessing and division into training and test sets.
- Step 2: Initialization of model parameters, including the number of nodes in the input and output layers of the LSTM neural network model, as well as parameters such as population size, shrinkage expansion coefficient, and the number of iterations for the QPSO algorithm.
- Step 3: Assignment of initialized particle population positions for the hidden layer of the LSTM neural network ( $n$ ), learning rate ( $\eta$ ), and the number of iterations (epoch). Training samples are then inputted into the LSTM network model for training.
- Step 4: Calculation of the initial fitness size and determination of the initial individual optimal position  $P_{best}$  and the current global optimal position  $A_{best}$  using the value of the fitness function.
- Step 5: Calculation of the average optimal position  $Z_{best}$  and then updating of the positions of the particles according to Eq. (16).
- Step 6: Calculation of the fitness value of each particle to obtain a smaller fitness value, so as to adjust the individual optimal position of the particle and the global optimal position.
- Step 7: Evaluation of whether the QPSO algorithm has achieved the set target or met the termination condition of the iterative cycle based on the fitness value. If the condition is met, proceed to Step 6; otherwise, return to Step 3.
- Step 8: Usage of the parameters of the optimal particle population to set the parameters of the LSTM neural network model, and then training of the optimized model to finally obtain the current unbalance prediction results.

In summary, the algorithm flowchart for the QPSO-LSTM current balance timing prediction model is depicted in Fig. 4.



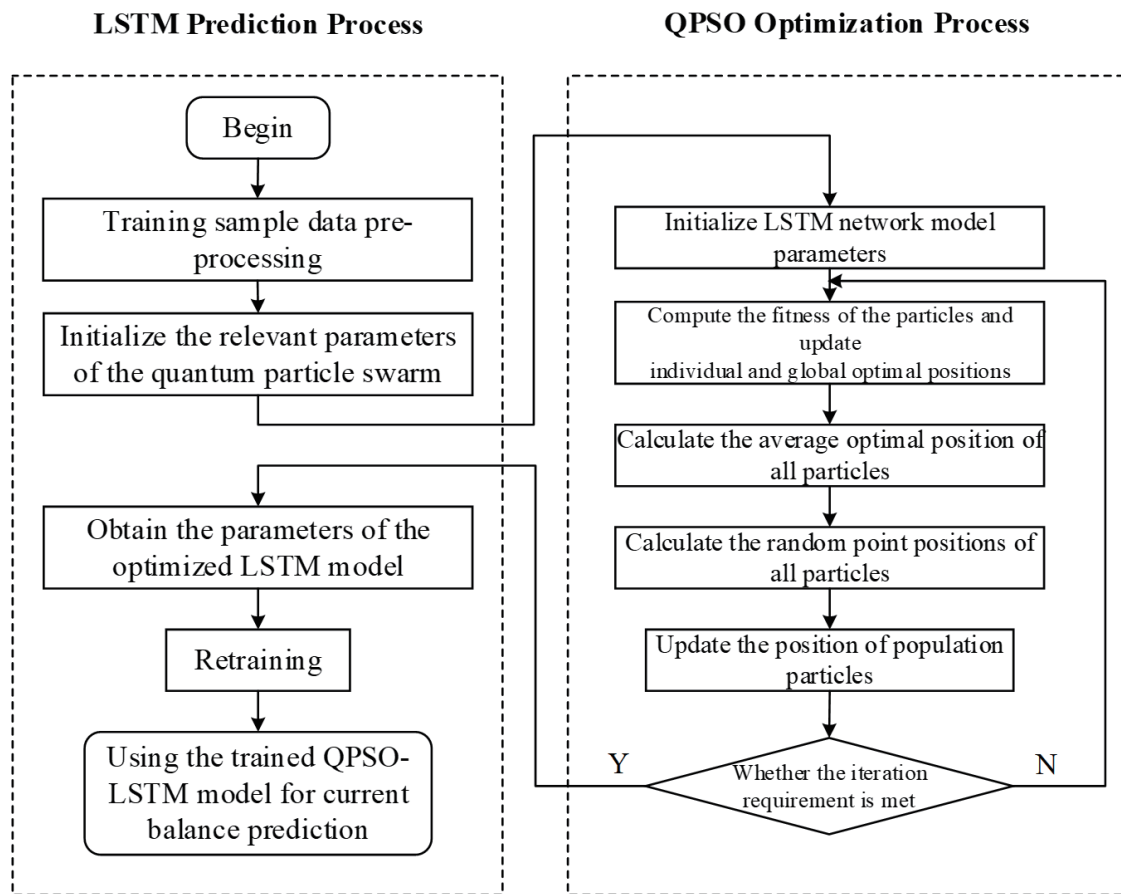


Fig. 4. Flow chart of QPSO-LSTM algorithm.

#### 4.2 Setting of QPSO-LSTM algorithm main parameters

In this study, every 1000 time-series data points in the established current unbalance dataset are selected as a set of sample objects, and a total of three data samples are divided into three groups for separate prediction. The acceleration constants  $c_1$  and  $c_2$  are set to 1.5 in the particle swarm algorithm, and the inertia weights of the swarm are linearly decreasing from 0.9 to 0.4. The shrinkage expansion coefficients of the quantum swarm are also linearly decreasing from 1 to 0.5. The simulation analysis yields the parameter space of this QPSO algorithm with the diagram of the seeking curve as shown in Fig. 5.

It can be seen from the graphs of the search curves that the PSO and QPSO algorithms have significant advantages in terms of convergence speed and search accuracy in finding the optimal solution, as the improved QPSO algorithm obtains results closer to the theoretical optimal solution by eliminating the particle's moving direction property and expanding the search space.

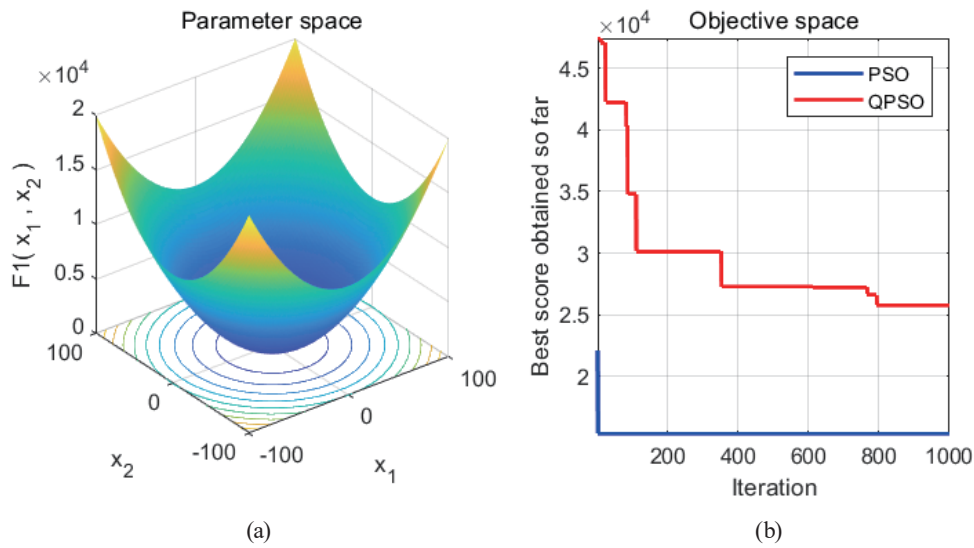


Fig. 5. (Color online) Parameter space and optimization-seeking curve diagram.

### 4.3 Prediction results of the model

On the basis of the set QPSO-LSTM parameters, the model is simulated and validated by combining the current balance timing datasets collected by the current sensor and preprocessed into training and test sets according to the ratio of 7:3. The LSTM and PSO-LSTM network models are also established to predict the same current unbalance timing data and further verify the capability of the QPSO-optimized LSTM network in current unbalance timing prediction. Prediction results are shown in Fig. 6.

From the prediction results, it is evident that the unoptimized LSTM network exhibits premature convergence and poor fitting results when used for predicting the timing of current balance. Conversely, the prediction results of the PSO-LSTM and QPSO-LSTM network models align closely with the actual current unbalance curve. Error comparison among the three models is presented in Table 1.

The comparison results show that the prediction results of the QPSO-LSTM network model are relatively more accurate. In summary, the QPSO-LSTM current unbalance timing prediction model established in this study has achieved high prediction stability and accuracy, and the LSTM network optimization method based on the QPSO algorithm has a significant improvement effect on the prediction accuracy.

### 4.4 Three-phase unbalance warning scheme based on time series prediction

On the basis of the timing prediction results of current unbalance, the unbalanced state of the three-phase four-wire system can be effectively detected. If the prediction indicates that the

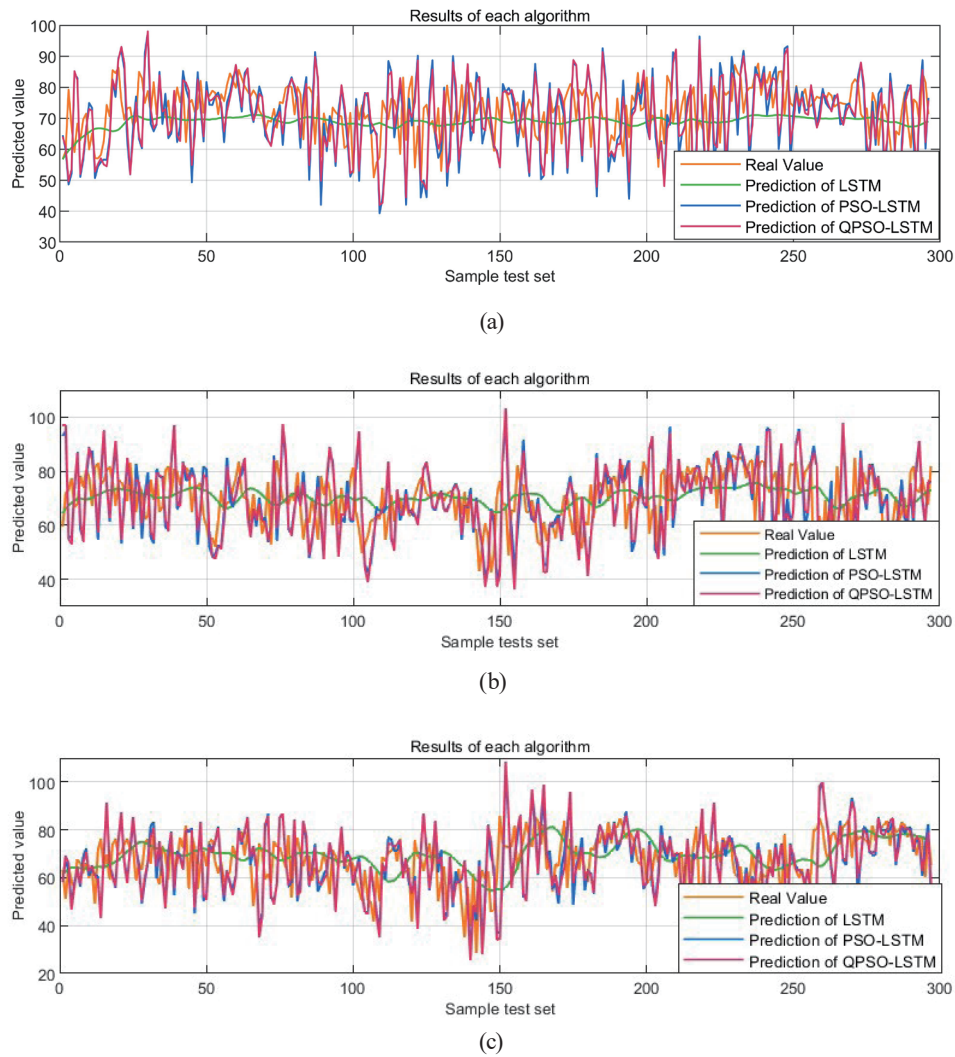


Fig. 6. (Color online) Comparison of prediction results. Datasets (a) I, (b) II, and (c) III.

Table 1  
Algorithm error comparison table.

Algorithm	Sample Object	$R^2$	$RMSE$	$MAE$	$MAPE$ (%)
LSTM	1	0.84035	12.5087	9.7785	13.7648
	2	0.86879	12.1533	9.3424	13.3211
	3	0.84565	12.3993	9.7543	13.6325
PSO-LSTM	1	0.88138	11.4783	9.0331	12.7241
	2	0.88646	11.3542	8.7351	12.3881
	3	0.87834	11.8726	8.9734	12.6186
QPSO-LSTM	1	0.93624	9.9308	7.5342	10.1092
	2	0.92778	9.3317	7.7735	10.2648
	3	0.93813	9.1231	7.7813	10.3169

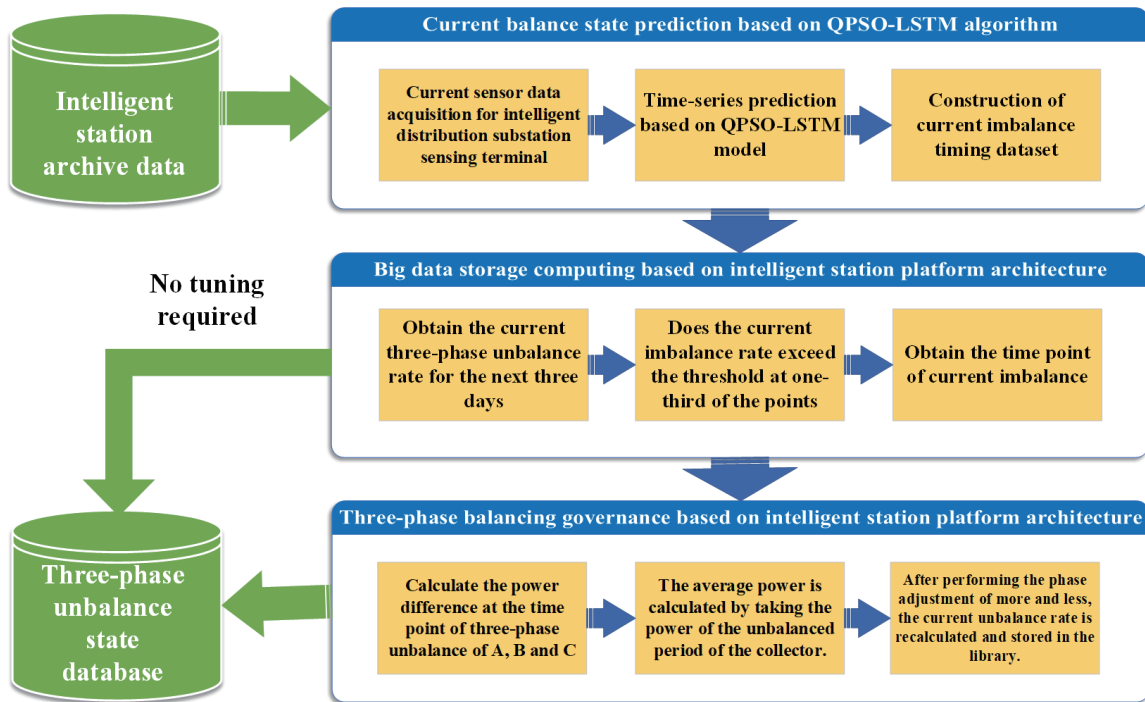


Fig. 7. (Color online) Three-phase unbalance warning control flow.

three-phase lines are likely to enter a continuous severe unbalanced state, a range of compensation methods and control devices are required to restore the three-phase balance. These methods include phase redistribution,<sup>(18)</sup> balance correction using multilevel converters,<sup>(19)</sup> and power control using AC to DC converters.<sup>(20)</sup>

To achieve efficient three-phase balancing control, the current sensor module of the intelligent distribution substation sensing terminal is utilized at various points in the distribution system. This targeted approach helps to minimize line loss and reduce the risk of faults. The specific process of the early warning control is illustrated in Fig. 7.

## 5. Conclusions

In this study, we first focused on collecting current data using the current sensor modules of power data collection terminals, such as the intelligent distribution substation sensing, branch line monitoring, and end sensing terminals of the three-phase four-wire distribution network. By combining data preprocessing and a three-phase current unbalance degree calculation model, we obtained a dataset for current unbalance rate timing. Furthermore, we developed a current balance timing prediction model based on the QPSO-LSTM algorithm. To improve the accuracy of the LSTM network prediction model, we utilized the properties of random space search in the QPSO algorithm. This enabled us to determine the optimal network layer weights and thresholds during training. As a result, we obtained a more precise prediction output function for the LSTM

network prediction model. Finally, we proposed a solution for three-phase balance state early warning control based on the time-series prediction results of the current unbalance degree. Note that the balance warning control method presented in this study for three-phase four-wire circuits demonstrates some feasibility. However, the current data collected by the current sensor still faces challenges such as insufficient accuracy and low reliability, which can negatively impact the prediction accuracy and timing prediction effectiveness. Nevertheless, the conceptual framework of the three-phase balance state early warning control, which relies on current sensor data fusion and QPSO-LSTM timing prediction, provides valuable insights for practical research on equipment rotation, load prediction control, and line loss metering in distribution network systems. Implementing this framework can help reduce energy loss in three-phase four-wire distribution networks and prevent the occurrence of severe faults.

### Acknowledgments

This work was supported by the science and technology project of Yunnan Power Grid Co., Ltd., which provided funding under project numbers YNKJXM20220010 and YNKJXM20210147.

### References

- 1 J. Chen, Q. Li, Y. Tang, and Y. Zhang: *Electr. Power Autom. Equip.* **4** (2022) 71. <https://doi.org/10.16081/j.epae.202201005>
- 2 C. Yang, S. Xia, N. Jiang, Y. Yi, K. Li, and C. Lin: *Autom. Instrum.* **2** (2022) 223. <https://doi.org/10.14016/j.cnki.1001-9227.2022.02.223>
- 3 K. Liu, D. Jia, W. Wang, G. Geng, and C. Wei: *Electr. Power Construct.* **10** (2021) 129. <https://doi.org/10.12204/j.issn.1000-7229.2021.10.014>
- 4 S. Hao, X. Cai, Y. Zhang, H. Liu, G. Chen, and X. Zhang: *Power Syst. Technol.* **4** (2021) 1547. <https://doi.org/10.13335/j.1000-3673.pst.2020.0216>
- 5 A. Bracale, P. Caramia, P. Falco, A. Fazio, and P. Varilone: *Int. J. Electr. Power Energy Syst.* **135** (2022) 107604. <https://doi.org/10.1016/j.ijepes.2021.107604>
- 6 R. Xie, F. Du, X. Cheng, Q. Zhou, and F. Xu: *Power Syst. Prot. Control* **21** (2020) 22. <https://doi.org/10.19783/j.cnki.pspc.191561>
- 7 Z. Zheng, B. Ye, K. Zhong, S. Yu, W. Shen, and Y. Yang: *Adv. Power Syst. Hydroelectr. Eng.* **1** (2023) 29. <https://doi.org/10.3969/j.issn.1674-3814.2023.01.004>
- 8 M. Li, S. Yu, and S. Wang: *Power Syst. Big Data* **5** (2022) 28.
- 9 T. Zhang, F. Guo, and J. Wang: *Electr. Eng.* **7** (2021) 48. <https://doi.org/10.3969/j.issn.1673-3800.2021.07.009>
- 10 F. Zhao, S. Li, X. Chen, Y. Wang, F. Zhang, X. Niu, and Y. Gan: *Power Syst. Technol.* **3** (2022) 870. <https://doi.org/10.13335/j.1000-3673.pst.2021.0413>
- 11 J. Yang, Y. Wang, and Z. Fang: *Electr. Eng.* **2** (2022) 26. <https://doi.org/10.3969/j.issn.1673-3800.2022.02.005>
- 12 X. An, T. Zhang, T. Li, J. Wang, T. Yong, and N. Jin: *Power Syst. Prot. Control* **13** (2020) 142. <https://doi.org/10.19783/j.cnki.pspc.190947>
- 13 Y. Li, C. Pan, H. Cao, N. Jin, and J. Wang: *Power Syst. Prot. Control* **12** (2020) 97. <https://doi.org/10.19783/j.cnki.pspc.190997>
- 14 F. Sun, J. Zhao, and N. Fu: *J. Henan Inst. Educ.* **4** (2022) 35. <https://doi.org/10.3969/j.issn.1007-0834.2022.04.006>
- 15 X. Wu, C. Dou, and D. Yue: *Electr. Power Syst. Res.* **199** (2021) 107398. <https://doi.org/10.1016/j.epsr.2021.107398>
- 16 W. Yang and Q. Li: *Strategic Study of CAE* **5** (2004) 87. <https://doi.org/10.3969/j.issn.1009-1742.2004.05.018>
- 17 S. Sun, Y. Wang, Y. Meng, C. Wang, and X. Zhu: *Energy Rep.* **8** (2022) 9899. <https://doi.org/10.1016/j.egy.2022.07.164>

- 18 V. Jimenez, A. Will, and D. Lizondo: Int. J. Electr. Power Energy Syst. **137** (2022) 107691. <https://doi.org/10.1016/j.ijepes.2021.107691>
- 19 Y. Yue, Q. Xu, P. Guo, X. Chu, Z. Shuai, and A. Luo: Int. J. Electr. Power Energy Syst. **129** (2021) 106729. <https://doi.org/10.1016/j.ijepes.2020.106729>
- 20 U. Kamnarn and V. Chunkag: Electr. Power Syst. Res. **77** (2007) 1585. <https://doi.org/10.1016/j.epsr.200611.005>

## About the Authors



**Qingchan Liu** was born in August 1982. He graduated from North China Electric Power University in 2012, majoring in electrical engineering, and is now a senior expert in the Metrology Center of Yunnan Power Grid Co., Ltd. (Yunnan Provincial Power Load Control Technology Center). His main research interests are in electric energy metering, intelligent energy measurement technology, and the online monitoring of the metering equipment operation status. ([zhizhe-520@163.com](mailto:zhizhe-520@163.com))



**Yuang Lin** was born in 2002 in Chaozhou City, Guangdong Province. Currently, he is a sophomore in the School of Information Engineering and Automation at Kunming University of Science and Technology and is pursuing a bachelor's degree in data science and big data technology with major research interests in artificial intelligence, data analytics, and data mining. ([18087147030@163.com](mailto:18087147030@163.com))



**Yao Zhong** was born in September 1983. He graduated from Wuhan University of Technology in 2008, majoring in test and measurement technology and instrumentation, and is now the senior manager of the Metrology Center of Yunnan Power Grid Co., Ltd. (Yunnan Provincial Power Load Control Technology Center). His main research interests are in electric energy metering and intelligent operation and maintenance. ([93336425@qq.com](mailto:93336425@qq.com))